All-fiber Optofluidic Biosensor

Yunbo Guo, Hao Li, Jing Liu, Karthik Reddy, and Xudong Fan

Department of Biomedical Engineering, University of Michigan, Ann Arbor, MI 48109-2099, USA

ABSTRACT

Optical fiber provides a unique and versatile platform for developing point-of-care optical sensing systems. Here we first propose a Fabry-Pérot (FP) based flow-through optofluidic biosensor, and then construct an all-fiber system which fully utilizes optical fibers to achieve rapid, sensitive, label-free biomolecular detection. This sensor consists of two single mode fibers (SMFs) with reflecting surfaces and a photonic crystal fiber (PCF) vertically sandwiched by them. Firstly, the SMFs act as waveguides for delivering light into and out of an optofluidic device (like PCF); secondly, instead of using the optical properties of the PCF, we take advantage of its inherent multiple fluidic channels and large sensing surface; thirdly, the two reflective surfaces and the PCF form a Fabry-Pérot microresonator and its resonance mode is sensitive to the change in the fluidic channels, which can be used to detect the substances flowing through the fluidic channels or adsorbing on the channel surface. In this paper, we explore the operating principle of the FP-based optofluidic biosensor, theoretically and experimentally investigate its feasibility and capability. The results show that the all-fiber optofluidic sensor is a promising technology platform for rapid, sensitive and high-throughput biological and chemical sensing.

Keywords: Optofluidic biosensor, fiber optic interferometer, photonic crystal fiber, flow-through, Fabry-Perot resonator, label-free, biomolecular detection, nanohole arrays

1. INTRODUCTION

Rapid and sensitive detection of unlabelled chemical and biological samples is of great interest in a variety of fields, including biomedical research, pharmaceutical discovery, environmental monitoring and homeland security, etc [1]. To date a number of optical label-free biosensors have been implemented to detect various biomolecules in different media, however, they suffer from either the detection limit bottleneck on the order of 1 pg/mm^2, or analyte (mass) transport limitations, or both [2,3]. For example, the nanoporous silicon based biosensor, utilizing 3-dimensional (3-D) detection in contrast to planar surface in most biosensors, significantly increases the sensing area and enhances the detection sensitivity [4-7]. However, due to dead-ended pores, it takes extremely long time for analytes to diffuse into (and out of) the porous detection region [4, 7], which also comprises its excellent sensitivity as a large fraction of binding sites on the nanoporous surface may not be utilized within a given detection time.

To address the slow analyte delivery issue in nanostructured sensors and inefficient mass transport problem in other surface (flow-over) based sensors, the flow-through scheme based on nanohole array sensors, using nanoholes as nanofluidic channels, has become a growing niche and been employed to enable rapid and efficient targeted delivery of analytes to the sensing area [8-13]. In particular, the nanoplasmonic-nanofluidic sensors, using metallic nanohole arrays fabricated on thin suspended membranes (~ 100-200 nm) as flow-through surface-plasmon-resonance (SPR) sensing elements, have demonstrated 6~14 fold improvement in the mass transport rate [9, 13]. However, fabrication of those membranes and integration with external microfluidics are very complicated. Moreover, challenges exist to ensure the structural integrity of the fragile membranes, which is subject to relatively high pressure gradients required to drive the analytes flow through. Additionally the SPR-based sensors suffer from low Q-factors (thus low detection resolution) and short penetration depths (hard to detect large size molecules), which restricts their sensing performance.

In this paper, we propose a Fabry-Pérot (FP) based flow-through optofluidic sensor to overcome the aforementioned problems. As illustrated in Figure 1, the FP-based optofluidic sensor employs a capillary with many built-in micro/nano-sized flow-through holes as resonance cavity and fluidic channels. When the capillary is placed between two reflectors, a Fabry-Pérot microresonator forms and detects the analytes binding to the internal surface of the holes. Similar to nanoporous silicon biosensors, the micro/nanohole arrays provide large sensing surface area within a 3-D detection region, which greatly concentrates the analytes and enhances the detection sensitivity. These flow-through

Frontiers in Biological Detection: From Nanosensors to Systems III, edited by Benjamin L. Miller, Philippe M. Fauchet,
Proc. of SPIE Vol. 7888, 78880O · © 2011 SPIE · CCC code: 1605-7422/11/$18 · doi: 10.1117/12.876008

holes also act as inherent fluidic channels, enabling quick and controllable analyte delivery. In addition, the resonant laser light circulates inside the FP cavity, so the depth of interaction with analytes is totally decided by the hole sizes, which can be adjusted to accommodate a wide range of biological samples from small molecules to viruses.

Photonic crystal fiber (PCF) with many flow-through holes has been widely used for biosensors, including liquid refractive index (RI) detection[14, 15], gas detection [16], or Surface-Enhanced Raman Scattering (SERS) detection [17]. Most of these biosensors make use of its optical properties which are related to the change of the analytes. Here, we take advantage of its inherent multiple fluidic channels and large sensing surface-to-volume ratio, and simply use it as a flow-through capillary and to construct a robust all-fiber optofluidic biosensor together with fiber optic interferometry [18,19].

In the following, we first present the principle of the FP based flow-through optofluidic sensor, theoretically analyze its detection sensitivity. Then we experimentally demonstrate its feasibility and capability with bulk solvent solvent change and real-time biomolecular detection.

2. PRINCIPLE

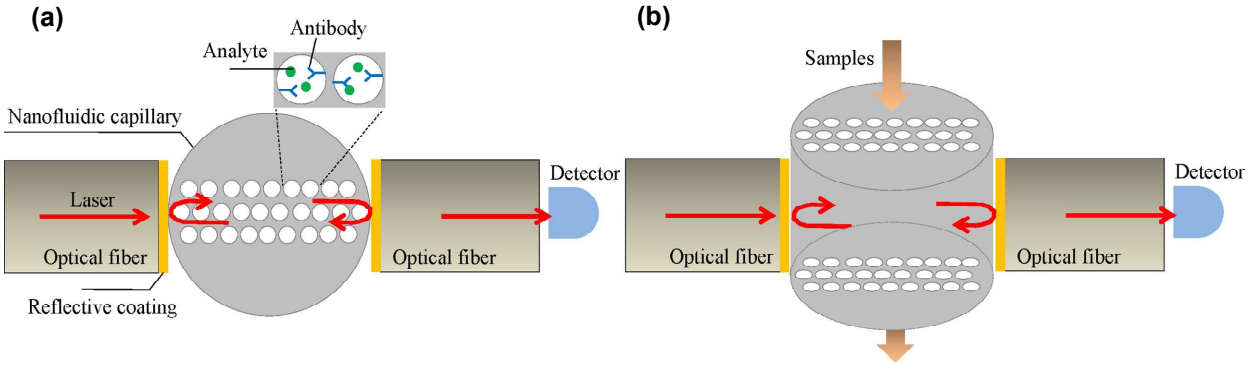

Fig. 1. Schematic illustration of the Fabry-Pérot based optofluidic biosensor using flow-through micro-sized capillary with micro/nanohole arrays as resonance cavity and fluidic channels. The analyte is bound to the ligand immobilized on the inner sensing surface of the holes. (a) Top view. (b) Side view.

Figure 1 (a) shows the schematic of the Fabry-Pérot based flow-through optofluidic sensor as described above. From the sake of simplicity, we first consider a one-dimensional Fabry-Pérot microcavity. As shown in Figure 2, the resonant cavity is composed of N flow-through holes with uniform hole size d and wall thickness t, which provides $2N$ solid-liquid interface for biomolecular adsorption.

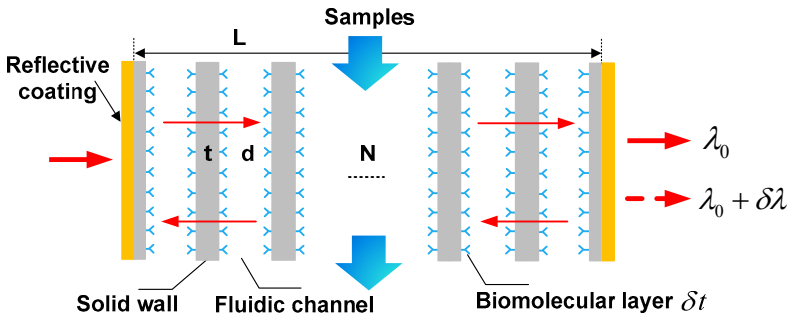

Fig. 2. Schematic of one-dimensional Fabry-Pérot resonator using flow-through multiple hole arrays as fluidic channels. The resonance wavelength shifts with the biomolecular binding to the inner walls.

The initial resonance wavelength λ_0 is determined by the following resonant condition:

$$2nL = m\lambda_0 \quad (m = 1,2,3...) \qquad (1)$$

where n and L are the effective refractive index (RI) and length of the cavity, respectively.

After the attachment of biomolecules, a molecule layer forms on both sides of each solid wall, which changes the resonant condition to:

$$2(nL + 2N \cdot \Delta n \cdot \delta t) = m(\lambda_0 + \delta\lambda) \qquad (2)$$

where Δn is the refractive index difference between the biomolecule and the ambient medium within the fluidic channels (e.g. water), δt is the effective thickness of the adsorbed biomolecular layer, and $\delta\lambda$ represents the shift of the resonant wavelength. Therefore, the surface detection sensitivity $\delta\lambda/\delta t$ is given by:

$$\frac{\delta\lambda}{\delta t} = 2N \cdot \frac{\Delta n}{nL} \cdot \lambda_0 \qquad (3)$$

As compared to a typical Fabry-Pérot based sensor having only one sensing surfaces [20], obviously the sensitivity is enhanced *2N*-fold in the FP-based optofluidic sensor.

The actual flow-through micro/nanohole arrays are 3-dimensional structure. A more generalized expression for the surface detection sensitivity can be deduced by considering the mode spectral shift caused by the fractional electro-magnetic energy change inside the cavity due to the biomolecular attachment [21, 22]:

$$\frac{\delta\lambda}{\delta t} = \frac{A}{V} \cdot \frac{\Delta n}{n} \cdot \lambda_0 \qquad (4)$$

where V and A are the total volume and internal surface area within the Fabry-Pérot cavity, respectively. Equation (4) shows the surface sensitivity is linearly proportional to the surface-to-volume ratio A/V. Note that Equation (4) is equivalent to Equation (3) discussed above.

Similarly, the bulk refractive index sensitivity (assuming that the RI of all fluidic channels is homogeneously changed), $\delta\lambda/\delta n$, can be derived as:

$$\frac{\delta\lambda}{\delta n} = \frac{W}{nV} \cdot \lambda_0 \qquad (5)$$

where W is the total volume of the fluidic channels within the Fabry-Pérot cavity. The bulk RI sensitivity can be used to characterize the capability of detecting large biomolecules (such as virus) which evanescent field based sensors are hard to handle.

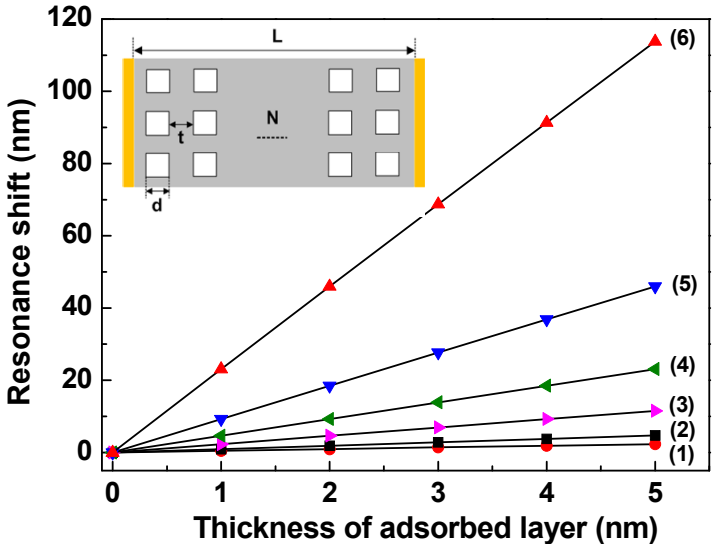

Fig. 3. Simulation of the sensor's spectral shift as a function of the adsorbed layer thickness for different hole sizes based on Eq. (4). Holes are square and the wall thickness t is the same as the hole size d. d =1, 0.5, 0.2, 0.1, 0.05, 0.02 μm for Curves (1)-(6). λ_0=1550 nm, Δn= 0.2, L=100 μm. The inset illustrates the hole arrangement.

Figure 3 plots the simulation results based on Eq. (4) for a FP cavity with square holes. In simulations, the length of the FP cavity is fixed to be 100 μm, and each hole has the same thickness as the solid wall (i.e. $d = t$). Therefore, when the hole size d is 1, 0.5, 0.2, 0.1, 0.05, 0.02 μm, the corresponding number of holes N within the resonance cavity is 50, 100, 250, 500, 1000 and 2500, respectively. With the decreased hole size, more holes and hence more surface area can be placed inside the cavity, resulting in a larger surface detection sensitivity. For the hole size from 1 μm to 20 nm, the sensitivity of 0.47 nm/nm to 23 nm/nm can be achieved. The sensitivity for the 20 - 100 nm holes is on par with the nanoporous silicon sensor with the similar pore sizes [5], but much larger than nearly all other types of label-free sensors such as surface plasmon resonance (SPR) based sensors, photonic crystal sensors, and ring resonator sensors [2].

3. EXPERIMENTS

3.1 Experimental setup

To experimentally verify the feasibility and capability of the Fabry-Pérot based flow-through sensor, we built a robust all-fiber optical system as Figure 4 (a) and (b) shows. We use a piece of commercialized PCF (F-AIR-10/1060 from Newport) with 124-μm outer diameter, a 10-μm hollow core, and 294 small holes (2.5-μm diameter), whose structure is shown in Figure 4 (c). The PCF is placed between two conventional SMF-28 single mode optical fibers with 3-nm-thick gold layer thermally evaporated on the silica fiber tip via 1 nm Chromium as adhesive layer. These two fibers provide a certain reflection and form a simple but effective FP interferometer. The light from a tunable laser source (1520 nm to 1570 nm) is directly coupled into one fiber, and the transmitted light is collected by the other one and then detected by a photodetector. In the following experiments, we used a 1-cm long PCF as the flow-through fluidic channels. Its two ends are connected with plastic tubes, and the analyte solution is withdrawn into and out of the PCF with 1 μL/min flow rate.

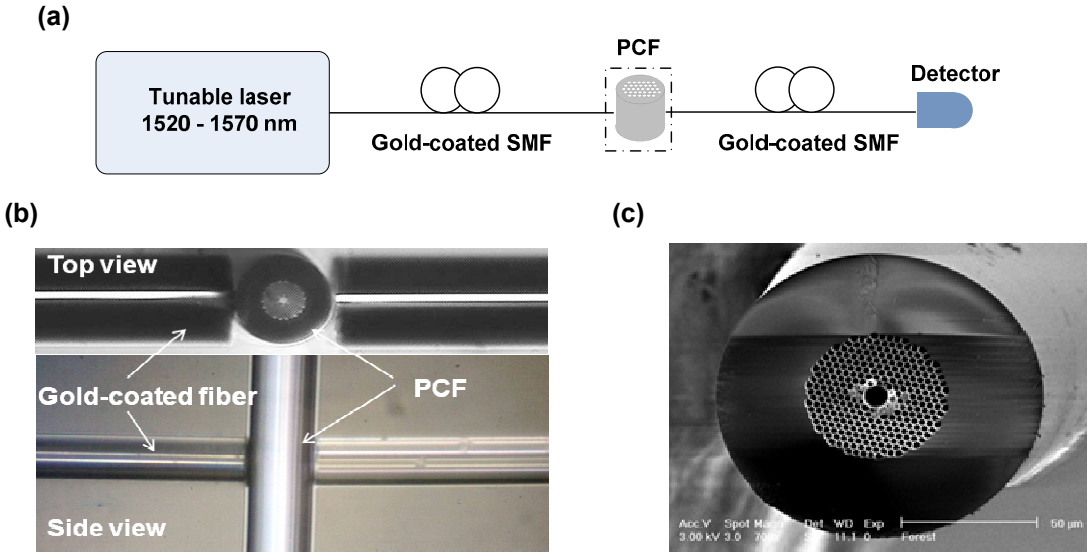

FIG. 4. (a) Schematic of the experimental setup. (b) Picture of the dotted square in (a) shows the Fabry-Pérot resonator consisting of a sandwiched by two gold-coated single mode fibers. (c) Scanning electron microscopy images of original photonic crystal fiber.

3.2 Experiments with original PCF

Figure 5 shows the transmission spectra of the all-fiber optofluidic sensor in the absence and presence of the original PCF (filled with DI-water). The presence of the PCF increases the cavity optical length, thus resulting in a smaller free spectral range. Note that even with hundreds of holes inside the cavity, the FP resonance still persists with a full-width-at-half-maximum (FWHM) of about 7.6 nm (obtained by Lorentz fitting), corresponding to a Q-factor of 200 (much higher than other flow-through sensors [9, 13]). The Q-factor can significantly be improved in the future by using a collimated beam instead of the diverging beam from the fiber [23] and highly-reflective dielectric multilayers instead of the lossy gold film [20, 24]. Note that the resonances observed in Fig. 5(a) are not due to the photonic band gap effect

resulting from the orderly arranged holes [14]. Randomly distributed holes in our sensor should work just well, like in a nanoporous silicon sensor.

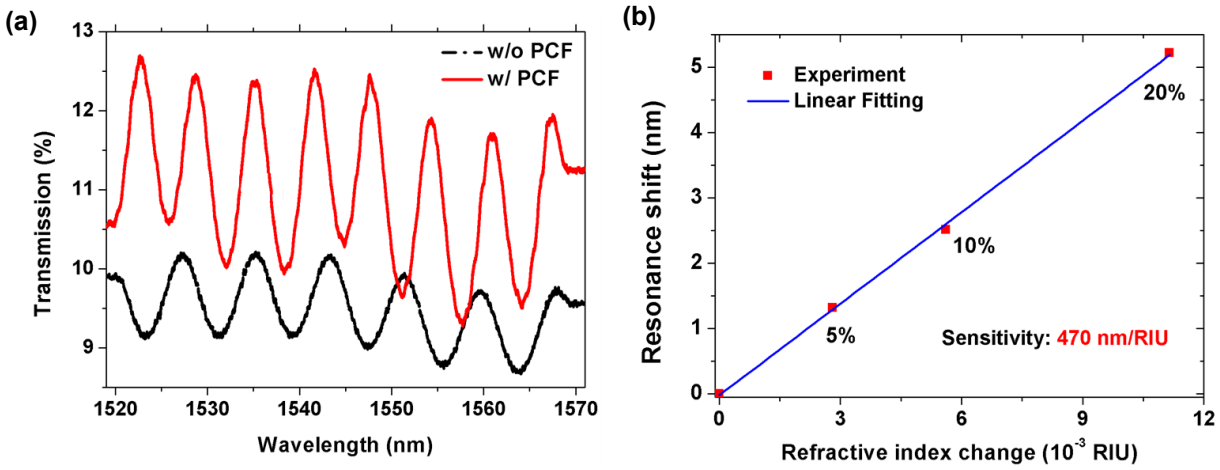

Fig. 5. (a) Transmission spectra of the all-fiber optofluidic sensor in response to the absence/presence of the PCF. (b) Characterization of the sensor's bulk solvent sensitivity with different refractive indices.

For characterization of the all-fiber optofluidic biosensor, we tested the sensor sensitivity to bulk solvent change. As Figure 5 (b) shows, a series of concentration ethanol solutions with different refractive indices are tested and a shift to a longer resonance wavelength was observed in response to the refractive index increasing within the PCF. A sensitivity of 470 nm/RIU (refractive index units) was obtained by measuring the slope of the resonant wavelength shift versus RI change.

3.3 Experiments with etched PCF

In order to improve the detection sensitivity, we consider etching off part of the cladding of the PCF. In this way, the surface-to-volume ratio A/V and W/V both increase, and the effective refractive index n decreases. According to Equations (4) and (5), both of the surface detection sensitivity and bulk solvent sensitivity will increase.

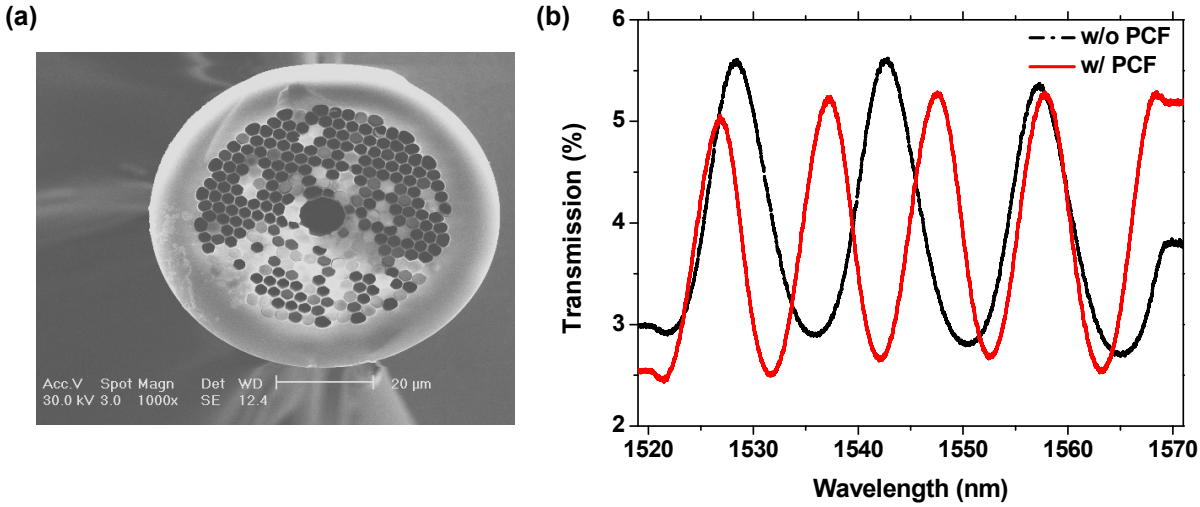

Fig. 6. (a) SEM image of the etched PCF. (b) Transmission spectra of the sensor with or without etched PCF.

As illustrated in Figure 6(a), the etched PCF has an outer diameter of 70 μm (reduced from 124 μm), but keeps the same fluidic holes. Figure 6 (b) shows the transmission spectra of the sensor with/without the etched PCF. Its resonance mode has a FWHM of 12 nm, which is wider than that in the original PCF. However, the sensor's sensitivity is greatly improved. In order to demonstrate this, we first tested its bulk solvent sensitivity. Figure 7 (a) shows the real-time spectral measurements with 0 to 5% ethylene glycol solutions flowing through the etched PCF consecutively with a rinsing step (by DI-water) between each new concentration to ensure the surface was cleaned before the next measurement. Figure 7 (b) showed the bulk solvent sensitivity of 780 nm/RIU, much larger than that achieved in the original PCF. It also represents the highest bulk sensitivity in the flow-through sensors [12,13].

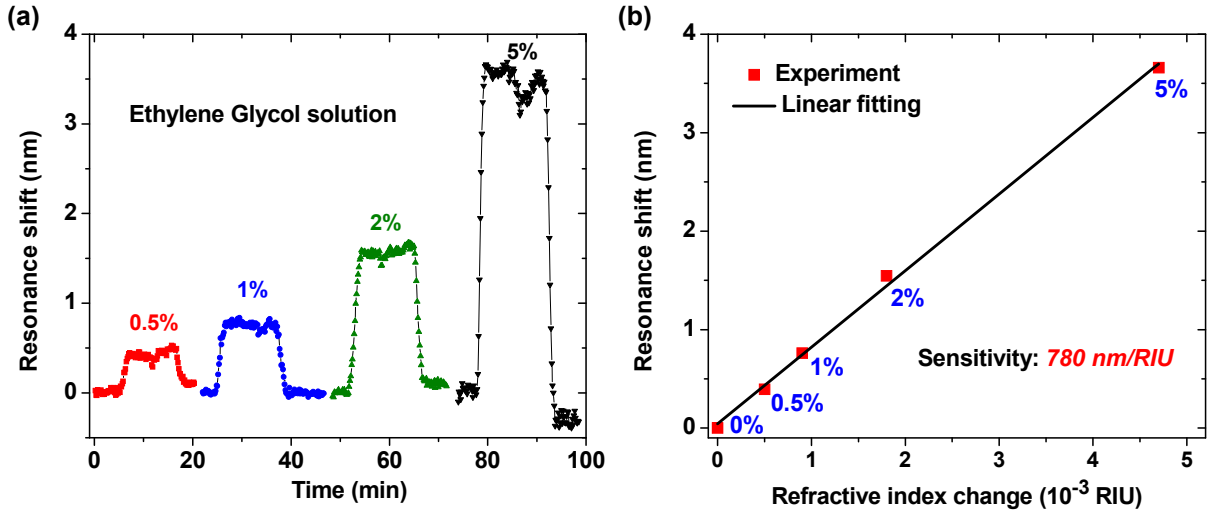

Fig.7. (a) Sensorgram of different concentrations ethylene glycol solution flowing through the etched PCF.
(b) Characterization of the sensor's bulk solvent sensitivity with different refractive indices.

An important application of biosensors is small-molecule detection. Here we use silica molecule with a molecular weight (MW) of 60 Da as a model, and measure the sensor response when low concentration (1%) aqueous hydrofluoric acid (HF) is flowing through the etched PCF and etching silica sensing surface [25]. Figure 8 shows the real-time spectral shift due to silica molecules continuously removed from the internal surface of the fluidic channels. The total resonance wavelength blueshift is 3.9 nm within 10 minutes etching time, which means that the optofluidic sensor is sensitive to the detachment of small molecule.

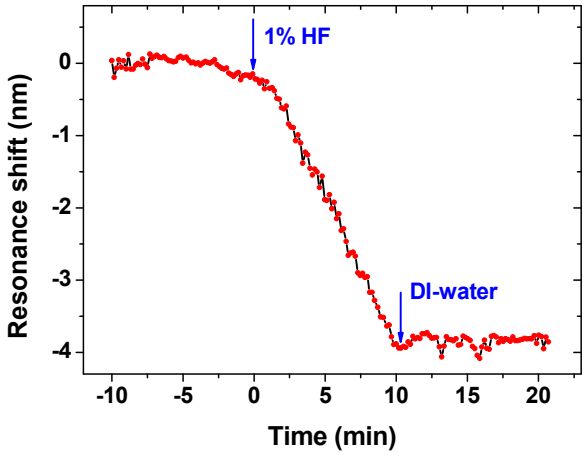

Fig. 8. Resonance shift in spectral position over time with 1% HF etching silica off the inner walls of the PCF.

4. CONCLUSIONS

In conclusion, we have proposed and demonstrated a Fabry-Pérot based flow-through optofluidic biosensor with multiple holes as the resonance cavity and fluidic channels. A robust all-fiber sensing system was built with a photonic crystal fiber and two gold-coated SMF fibers, which exhibited rapid analyte delivery, high sensitivity (780 nm/RIU) and capability of small molecule detection. Further improvements of this sensor are expected to yield even higher performance. First, the mass transport rate can be dramatically increased by shortening the PCF length (like 1 mm) and by combining other fluidic control methods [8, 26]. Second, the detection sensitivity of the FP-based optofluidic biosensor can be greatly improved by using structures with large number of holes, like micro/nanostructured capillary (see more details in our recent work [27]). Third, since this sensor is also able to be operated with intensity measurement at a single wavelength, the detection resolution can be improved to 10^{-5} nm [28]. Fourth, the FP resonator can be built with optical fibers, waveguides, etc, which makes it much easier for system integration and can be scaled up to an array format for multiplexing detection. By all important metrics for sensing, we anticipate that the Fabry-Pérot based flow-through optofluidic biosensor will provide rapid, sensitive, high-throughput, label-free detection for biological and chemical applications.

REFERENCES

[1] Narayanaswamy, R., and Wolfbeis, O. S., [Optical Sensors: Industrial, Environmental and Diagnostic Applications] Springer, New York(2004).

[2] Fan, X., White, I. M., Shopova, S. I., Zhu, H., Suter, J. D., and Sun, Y., "Sensitive optical biosensors for unlabeled targets: A review," Anal. Chim. Acta. 620, 8-26 (2008).

[3] Hunt, H. K., and Armani, A. M., "Label-free biological and chemical sensors," Nanoscale 2, 1544-1559 (2010).

[4] Chan, S., Fauchet, P. M., Li, Y., Rothberg, L. J., and Miller, B. L., "Porous silicon microcavities for biosensing applications," Phys. Stat. Sol. A 182, 541-546 (2000).

[5] Ouyang, H., Striemer, C. C., and Fauchet, P. M., "Quantitative analysis of the sensitivity of porous silicon optical biosensors," Appl. Phys. Lett. 88, 163108 (2006).

[6] Lin, V. S.-Y., Motesharei, K., Dancil, K.-P. S., Sailor, M. J., and Ghadiri, M. R., "A Porous Silicon-Based Optical Interferometric Biosensor," Science 278, 840-843 (1997).

[7] Orosco, M. M., Pacholski, C., and Sailor, M. J., "Real-time monitoring of enzyme activity in a mesoporous silicon double layer," Nature Nanotechnol. 4, 255-258 (2009).

[8] Sinton, D., Gordon, R., and Brolo, A. G., "Nanohole arrays in metal films as optofluidic elements: progress and potential," Microfluid. Nanofluid. 4, 107-116 (2008).

[9] Eftekhari, F., Escobedo, C., Ferreira, J., Duan, X., Girotto, E. M., Brolo, A. G., Gordon, R., and Sinton, D., "Nanoholes As Nanochannels: Flow-through Plasmonic Sensing," Anal. Chem. 81, 4308-4311 (2009).

[10] Escobedo, C., Brolo, A. G., Gordon, R., and Sinton, D., "Flow-Through vs Flow-Over: Analysis of Transport and Binding in Nanohole Array Plasmonic Biosensors," Anal. Chem. 82, 10015-10020 (2010).

[11] Gordon, R., Brolo, A. G., Sinton, D., and Kavanagh, K. L., "Resonant optical transmission through hole-arrays in metal films: physics and applications," Laser Photon. Rev. 4, 311-335 (2010).

[12] Huang, M., Yanik, A. A., Chang, T.-Y., and Altug, H., "Sub-Wavelength Nanofluidics in Photonic Crystal Sensors," Opt. Express 17, 24224-24233 (2009).

[13] Yanik, A. A., Huang, M., Artar, A., Chang, T.-Y., and Altug, H., "Integrated nanoplasmonic-nanofluidic biosensors with targeted delivery of analytes," Appl. Phys. Lett. 96, 021101 (2010).

[14] Domachuk, P., Nguyen, H. C., Eggleton, B. J., Straub, M., and Gu, M., "Microfluidic tunable photonic band-gap device," Appl. Phys. Lett. 84, 1838-1840 (2004).

[15] Wu, D. K. C., Kuhlmey, B. T., and Eggleton, B. J., "Ultrasensitive photonic crystal fiber refractive index sensor," Opt. Lett. 34, 322-324 (2009).

[16] Benabid, F., "Hollow-core photonic bandgap fibre: new light guidance for new science and technology," Philosophical Transactions of the Royal Society A: Mathematical, Physical and Engineering Sciences 364(1849), 3439-3462 (2006).

[17] Han, Y., Tan, S., Oo, M. K. K., Pristinski, D., Sukhishvili, S., and Du, H., "Towards Full-Length Accumulative Surface-Enhanced Raman Scattering-Active Photonic Crystal Fibers," Advanced Materials 22, 2647-2651 (2010).

[18] Song, W. Z., Zhang, X. M., Liu, A. Q., Lim, C. S., Yap, P. H., and Hosseini, H. M. M., "Refractive index measurement of single living cells using on-chip Fabry-Pérot cavity," Appl. Phys. Lett. 89, 203901 (2006).
[19] Domachuk, P., and Eggleton, B. J., "Fiber-based optofluidics," Proc. SPIE 6588, 65880C-12 (2007).
[20] Bergstein, D. A., Ozkumur, E., Wu, A. C., Yalcin, A., Colson, J. R., Needham, J. W., Irani, R. J., Gershoni, J. M., Goldberg, B. B., DeLisi, C., Ruane, M. F., and Ünlü, M. S., "Resonant cavity imaging: A means toward high-throughput label-free protein detection," IEEE J. Sel. Top. Quan. Electron. 14, 131-139 (2008).
[21] Arnold, S., Khoshsima, M., Teraoka, I., Holler, S., and Vollmer, F., "Shift of whispering-gallery modes in microspheres by protein adsorption," Opt. Lett. 28, 272-274 (2003).
[22] Arnold, S., Ramjit, R., Keng, D., Kolchenko, V., and Teraoka, I., "Microparticle photophysics illuminates viral bio-sensing," Faraday Discuss. 137, 65-83 (2008).
[23] Jiang, Y., and Tang, C., "High-finesse micro-lens fiber-optic extrinsic Fabry–Perot interferometric sensors," Smart Mater. Struct. 17, 055013 (2008).
[24] Pruessner, M. W., Stievater, T. H., and Rabinovich, W. S., "Integrated waveguide Fabry-Perot microcavities with silicon/air Bragg mirrors," Opt. Lett. 32, 533-535 (2007).
[25] White, I. M., Hanumegowda, N. M., and Fan, X., "Subfemtomole detection of small molecules with microsphere sensors," Opt. Lett. 30, 3189-3191 (2005).
[26] Mawatari, K., Tsukahara, T., Sugii, Y., and Kitamori, T., "Extended-nano fluidic systems for analytical and chemical technologies," Nanoscale 2, 1588-1595 (2010).
[27] Guo, Y., Li, H., Reddy, K., Shelar, H. S., Nittoor, V. R., and Fan, X., "Optofluidic Fabry-Pérot cavity biosensor with integrated flow-through micro/nano channels," Submitted.
[28] Guo, Y., Ye, J. Y., Divin, C., Huang, B., Thomas, T. P., Baker, J. J. R., and Norris, T. B., "Real-Time Biomolecular Binding Detection Using a Sensitive Photonic Crystal Biosensor," Anal. Chem. 82, 5211-5218 (2010).